Physicochem. Probl. Miner. Process., 60(3), 2024, 189757

http://www.journalssystem.com/ppmp

Physicochemical Problems of Mineral Processing

ISSN 1643-1049

Study on the mechanism of controlling the morphology of basic magnesium carbonate prepared under different hydration conditions

Yang Yang [1,3], Limei Bai [1,3], Yuxin Ma [1,3], Yulian Wang [2]

[1] North China University of Science and Technology, Tangshan 063210, China

[2] Shenyang University of Science and Technology, Shenyang 110159, China

[3] Collaborative Innovation Center for Green Development and Ecological Restoration of Mineral Resources, Tangshan 063210, China

Corresponding author: limeibai@126.com (Li Mei Bai)

Abstract: Basic magnesium carbonate is gaining prominence in flame retardant materials due to its excellent flame-retardant properties and clean decomposition products. This study investigates a hydration-carbonation method to address challenges related to the preparation, morphology control, and stability of magnesium basic carbonate. The impact of hydration conditions on the morphology of the carbonate was analyzed using scanning electron microscopy (SEM) and X-ray diffraction (XRD). The results indicate that spherical magnesium basic carbonate with regular morphology and uniform particle size can be achieved at a hydration temperature of 50°C for 1.5 hours. However, extending the hydration time and increasing the temperature resulted in irregular morphologies. Molecular dynamics simulations using the CASTEP and Forcite modules of Materials Studio were employed to understand the influence of hydration-carbonation conditions on the carbonate's morphology. The simulations revealed that the (1 1 1) and (2 0 0) crystal faces of MgO, with higher surface energies, promote the formation of precursor magnesium hydroxide nuclei, leading to heterogeneous magnesium alkali carbonate at elevated temperatures. Prolonged hydration time resulted in fragmented carbonate structures. To control the morphology of magnesium alkali carbonate, it is essential to optimize hydration temperature and duration. The simulation results corroborate experimental findings, providing deeper insights into the liquid-gas-solid adsorption relationships during the carbonation process. This study offers valuable guidelines for the controlled synthesis of magnesium basic carbonate, enhancing its applicability in flame retardant materials.

Keywords: alkaline magnesium carbonate, conformational control, simulation, carbonation treatment, molecular dynamics, surface energy

1. Introduction

With the advancement of materials science and the increasing emphasis on environmental protection, inorganic flame retardants are being used more frequently due to their high efficiency and environmental friendliness. Magnesium carbonate is recognized as a stable inorganic hydrate flame retardant. It has the advantages of high decomposition temperature, heat absorption during decomposition, non-toxicity and non-pollution, recyclability, low preparation cost, and non-flammability of decomposition products water and carbon dioxide. While the carbonization method has the advantages of high purity and carbon sequestration, direct preparation often leads to surface polarity in the preparation of basic magnesium carbonate, resulting in severe agglomeration. This complicates the filtration process during preparation and leads to poor compatibility with non-polar polymers, ultimately limiting the mechanical and processing properties of magnesium alkali carbonate derived polymers (Wang et al., 2020). The carbonization of Mg hydroxide is less efficient when using the carbonization method, and the use of defective Mg hydroxide feedstock is more favorable for the carbonization reaction (Wu et al., 2021). Furthermore, carbonization can be employed as a direct air capture technology for the purpose of capturing CO_2 from flue gas, the atmosphere, and indoor air. The CO_2 capture efficiency of direct air capture by slurry-based MgO nanosorbents can be enhanced by the

DOI: 10.37190/ppmp/189757

application of an external force during the wet carbonization process (Kyungil et al., 2023). However, lightly charred powders often contain impurities, the decontamination process is time-consuming, and the use of other decontamination methods may introduce new impurities. To improve the yield of carbonation methods, the crystal structure of basic magnesium carbonate must be adjusted to minimize agglomeration and surface polarity. The focus of this study is on the carbonization process for the production of basic magnesium carbonate.

To address the issue of unstable morphology and particle size during the preparation of alkali carbonate using the carbonization method, Zhang et al. (2008) and others controlled the pyrolysis temperature and successfully produced rod, flake, and petal-like alkali magnesium carbonate. Zhao et al. (2017) and others substituted the magnesium source with magnesium sulfate and synthesized flaky, rose-patterned, rod-shaped basic magnesium carbonate. Chen et al. (2016) and others examined the variations in the crystal shape of basic magnesium carbonate prepared using urea, ammonium bicarbonate, and sodium bicarbonate as different alkali sources, and the impact of different magnesium sources on the morphology of basic magnesium carbonate. Wang et al. (2020) and others used sodium stearate to adjust the hydrophobicity of magnesium carbonate and enhance its surface properties. Sato et al. (2020) and others investigated the process of carbon dioxide fixation by serpentine in a hydrothermal environment. They produced alkaline magnesium carbonate under acidic conditions with a pH of 1.0, explored carbonization without the need for serpentine acidification and decontamination additives, and improved the method for preparing magnesium carbonate. Schaef et al. (2011) and others observed the carbonation reaction of hydromagnesite [$Mg(OH)_2$] at various temperatures using in-situ high-pressure X-rays. At 75°C, they discovered the formation of a magnesium carbonate product, confirming that carbon dioxide dissolved in water is essential for carbonation. Sun et al. (2015) and others utilized magnesium chloride and ammonia to synthesize rose-like basic magnesium carbonate with different particle sizes and achieved this by controlling the gas flow rate, reaction temperature, and initial concentration. Chen et al. (2017) and others reduced the crystal length of magnesium carbonate trihydrate by introducing nitrate and sulfate ions. Cheng et al. (2018) investigated the impact of ethanol on the crystallization and phase transition of $MgCO_3 \cdot 3H_2O$ in the $MgCl_2$-CO_2-NH_3-H_2O system and found highly dispersed and stable crystals of magnesium carbonate trihydrate at a 30% ethanol concentration. Stefánsson et al. (2017) and others used infrared spectroscopy and quantum mechanical density functional theory to examine the interaction between magnesium bicarbonate and carbonate ions in an aqueous solution. The researchers examined the relationship between the distribution of magnesium bicarbonate ions and the nucleation and early bonding of magnesium carbonate. The researchers mentioned above-synthesized magnesium basic carbonate by controlling the pyrolysis temperature, using various modifiers, and employing different sources of magnesium. They also controlled the morphology under these circumstances. However, there is still a need to investigate the morphology of the magnesium hydroxide precursor and its transformation into magnesium basic carbonate under various hydration conditions at atmospheric pressure.

Based on the above, to reduce processing costs and produce magnesium basic carbonate with regular morphology, this paper conducts a study on the hydration process of the raw material using the carbonation method of lightly burned powder. The study investigates the impact of hydration temperature and duration on magnesium basic carbonate. It also integrates molecular dynamics using CASTEP (Cambridge Sequential Total Energy Package) from Materials Studio. The surface energy of MgO, adsorption energy, and radial distribution function of hydration and carbonation models were simulated using CASTEP (Cambridge Sequential Total Energy Package), Forcite, and the Adsorption modules of Materials Studio. These simulations also investigated the energy of the preferred adsorption reaction on the crystal surface during the hydration and carbonation processes. The simulation results clarify experimental phenomena and provide a solid basis for optimizing the preparation conditions of the carbonation method.

2. Materials and methods

2.1. Materials

The raw material for this experiment, light calcined powder, was obtained from Liaoning. The chemical analysis and XRD results of the obtained samples are shown in Table 1 and Fig. 1, respectively.

Table 1 Chemical composition of lightly burned powder

Components	MgO	CaO	Fe_2O_3	Al_2O_3	SiO_2
Content(wt%)	92.49	1.13	0.61	0.77	5

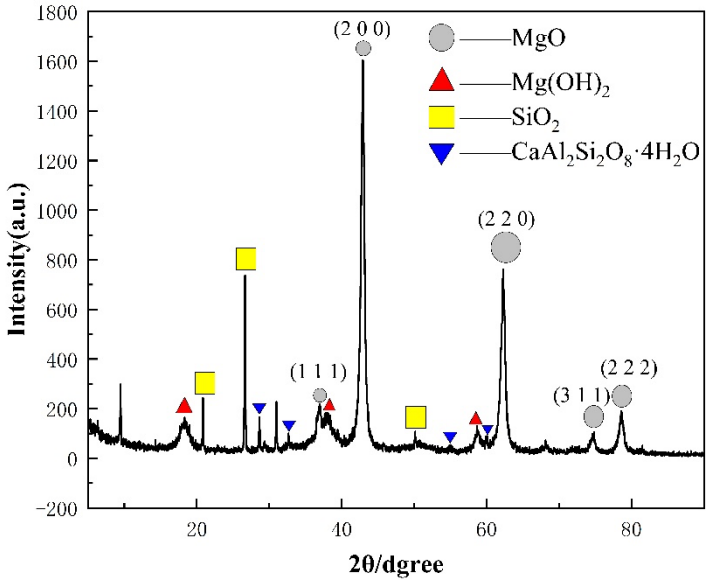

Fig. 1. XRD of lightly burned powder

From Table 1, it can be seen that the CaO, Fe_2O_3, and Al_2O_3 in the light-fired powder are less than 1.2%, of which MgO is as high as 92.49%, and its theoretical content is 95%. As can be seen from Fig. 1, the main diffraction peak of the light-fired powder is MgO, with high intensity and small half-peak width, the main impurity SiO_2 content of 5%, and the others are some of the more reactive MgO generated by water absorption of $Mg(OH)_2$ and very low content of aluminate minerals composed of heterogeneous peaks. Calcium oxides are often present as impurities since lightly fired powder is a product of magnesite processing (Huang, et al., 2021). In addition, different magnesite ore sources also affect the morphology and activity of the light-fired powder feedstock (Choudhary, et al. 1991). However, in the carbonation process, the pH of the subsequent carbonation is always higher than 7(In the pH interval 7.5 to 9.0 the main form of carbonate present is bicarbonate (Botha, et al., 2001)), so that impurities such as Ca and Fe are not soluble in the weak acid environment, thus achieving the separation of impurities.

2.2. Experimental methods

Firstly, an appropriate amount of slightly calcined powder was weighed and poured into a conical flask, poured into a reactor and placed on a magnetic stirrer in the ratio of m(MgO):m(H2O) 1:40, then stirred at different speeds and reacted for different times at a certain temperature to obtain different degrees of hydration of magnesium oxide/magnesium hydroxide hybrid precursors(Due to the different hydration conditions, the thickness of the magnesium hydroxide formed in the surface layer of the magnesium oxide is also different, so there is a difference in the magnesium hydroxide content). The precursors were allowed to cool to room temperature, and then carbon dioxide was introduced at a rate of 0.1 L/min for 40 min at room temperature, and the low activity unhydrated magnesium oxide was filtered off to obtain magnesium bicarbonate ($Mg(HCO_3)_2$) solution at the end of carbonation. Finally, the prepared $Mg(HCO_3)_2$ solution was put into a conical flask and placed on a magnetic stirrer, and the pH was adjusted with 5 mol/L NaOH solution. Since the change of pH affects the morphology of the basic magnesium carbonate ergo (Mitsuhashi, 2005), pyrolysis was carried out for 90 min in a water bath at 70 ℃ with pH fixed at 7.7. After pyrolysis was completed, the solution was placed in an oven at 50 ℃ to dry, and then subjected to XRD and SEM analysis, respectively.

Carbon dioxide and water molecule models were constructed using MS software, and model optimization was performed using the Geometry Optimization function of the Forcite module, and the

cell structure data (space groups, cell lengths, angles, and atomic coordinates) of magnesium hydroxide and magnesium alkali carbonate of type 4-1-4 were imported to obtain the corresponding crystal models. CASTEP crystal surface energy calculations were performed on each crystal surface of the original cell and cut magnesium oxide, respectively, and the surface energy of each crystal surface could be obtained by using the GGA-PBE method with the accuracy set to Fine. The water molecule and carbon dioxide molecule models were introduced into the models of magnesium hydroxide and 4-1-4 type alkaline magnesium carbonate, respectively, and the molecular dynamics simulation calculations were carried out by using the NVT method of Forcite Dynamics module with a step size of 0.01 fs at 288.15 K to obtain the corresponding radial distribution functions. The adsorption simulations of water molecules and carbon dioxide were then performed using the Adsorption Locator module to obtain the corresponding adsorption energies.

The cell structures of $Mg(OH)_2$ and $4MgCO_3 \cdot Mg(OH)_2 \cdot 4H_2O$ were obtained from ICSD (Inorganic Crystal Structure Database) (Fig. 2) and were used to start the subsequent adsorption modeling and energy calculations.

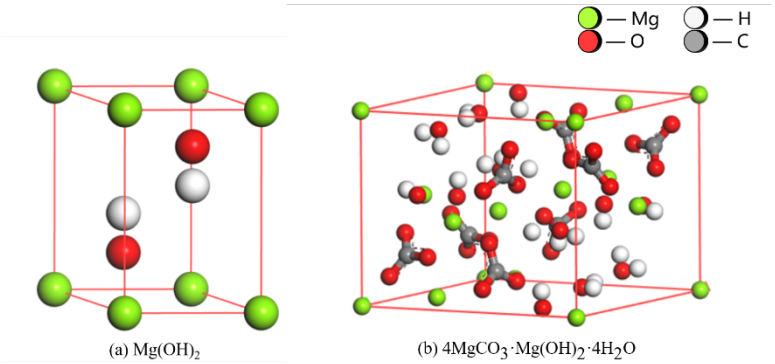

Fig. 2. Schematic diagram of a crystal cell

The corresponding process for producing basic magnesium carbonate by carbonization of lightly burned powder is as follows: magnesium oxide is hydrated, carbonized, and pyrolyzed to obtain the corresponding 4-1-4 type basic magnesium carbonate, and the specific reaction formula is as follows (Wang, et al., 2015):

$$MgO+H_2O \rightarrow Mg(OH)_2\downarrow \quad (1)$$

$$Mg(OH)_2+CO_2 \rightarrow Mg(HCO_3)_2 \quad (2)$$

$$Mg(HCO_3)_2+2H_2O \rightarrow MgCO_3 \cdot 3H_2O+CO_2\uparrow \quad (3)$$

$$5(MgCO_3 \cdot 3H_2O) \rightarrow 4MgCO_3 \cdot Mg(OH)_2 \cdot 4H_2O \quad (4)$$

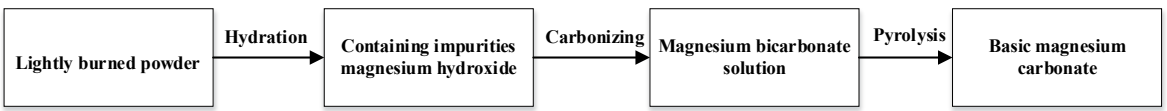

Fig. 3. Experimental process flow

It is important to note that the impurity-containing magnesium hydroxide is derived from the light-fired powder feedstock, and the impurity type is consistent with it. The impurity structure affects the distribution structure of the magnesium hydroxide layer, which affects the leaching rate, so the distribution of magnesium hydroxide impurities is consistent with the results of the subsequent leaching rate.

3. Results and discussion

A series of replicate tests were conducted at a magnesium oxide-to-water ratio of 1:40. The average concentrations of magnesium bicarbonate obtained at varying hydration temperatures and durations are presented below.

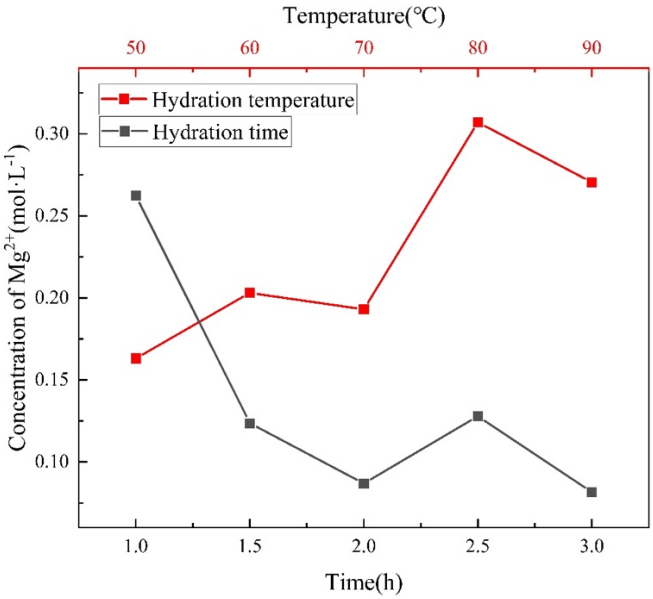

Fig. 4. Effect of hydration conditions on the concentration of magnesium ion

Fig. 4 shows that the concentration of magnesium ions is higher after a hydration period of 1 hour. An increase in temperature does not further enhance the concentration of magnesium bicarbonate. This may be due to the prolonged hydration time, which makes it difficult for magnesium hydroxide to carbonate and for a few crystal surfaces to continue growing, resulting in a larger exposed surface area and ultimately affecting the efficiency of carbonization. During the 1-hour hydration period, the precursor magnesium hydroxide formed from the hydration of magnesium oxide was imperfectly crystallized, leading to more uniformly exposed crystal surfaces. While MgO can weakly chemisorb CO_2 by forming an unilaterally stretched carbonate-like structure when added to H_2O, $Mg(OH)_2$ formed by the hydration of MgO only exhibits weak physical adsorption of CO_2, which is entirely due to dispersive forces. The composite of $MgO/Mg(OH)_2$ consists of MgO and $Mg(OH)_2$, both of which contain defects. The presence of water has a slight positive effect on adsorption. Defective $Mg(OH)_2$ significantly enhances the adsorption of CO_2 by enabling strong chemisorption of CO_2, leading to the formation of a carbonate-like structure (Wu et al., 2021). This results in a high concentration of magnesium bicarbonate within a short hydration period. The concentration was obtained by subtracting the remaining Mg from the total initial Mg (Zhu et al., 2017).

The concentration of magnesium bicarbonate increased as the hydration temperature rose, reaching 0.3 mol/L when the temperature exceeded 70 ℃. This phenomenon may be attributed to the accelerated growth of precursor magnesium hydroxide on all crystal surfaces at elevated temperatures, leading to the formation of smaller nuclei and higher density. This increases the contact area for carbonation and facilitates the carbonation reaction.

3.1. The impact of hydration duration on the morphological control of magnesium alkali carbonate during the hydration-carbonation process

The morphological changes of the magnesium alkali carbonate product obtained from carbonation and pyrolysis were examined under the conditions of a hydration temperature of 50°C and a stirring rate of 300 rad/min. The results are presented in the figures. Fig. 5 and 7 show the results for different hydration durations.

Fig. 5(a)-(e) displays the scanning electron microscope (SEM) images of magnesium carbonate samples obtained at different hydration times. The samples hydrated for 1.5 hours and 2 hours were spherical, while the samples under other conditions exhibited a fish scale pattern and fragmentation. Among the samples, the magnesium basic carbonate sample with a hydration duration of 1 hour may not have completed the crystallization of magnesium hydroxide due to the short duration. This incomplete crystallization may have resulted in incomplete carbonation, leading to a flaky texture and a more chaotic composition. With longer hydration time, the crystallization process becomes more

complete after 1.5 hours. The overall morphology exhibits a petal-like distribution, and individual crystals tend to be spherical. However, after 2.5 hours, the petal-like crystallization of the interlayer significantly increases and becomes thinner. During the 3-hour hydration process, the basic magnesium carbonate no longer exhibits a petal-like distribution and instead presents a flake-like distribution without any interspersed phenomenon between layers, as illustrated in Fig. 5(f). The particle size of magnesium alkali carbonate initially increases, followed by a decrease, and then increases again as the hydration time is prolonged.

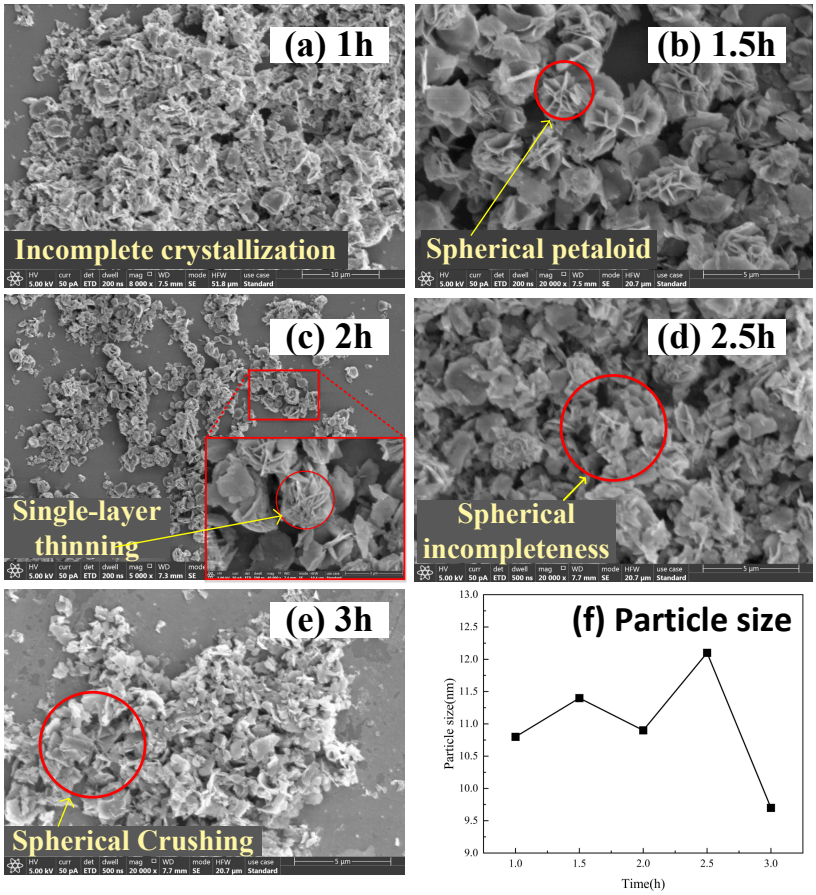

Fig. 5. SEM of alkaline magnesium carbonate at different hydration times

The EDS analysis results for the corresponding samples are shown in Fig. 6. In the energy range around 1.75 keV, there is a background peak corresponding to silicon, while the other major peaks are attributed to C, O, and Mg elements. The overall carbon content shows a trend of decreasing first and then increasing. The Mg element content is lowest at a hydration time of 1.5 hours, with magnesium mass fluctuating in the range of 16% to 22%.

The X-ray diffraction (XRD) patterns of the basic magnesium carbonate samples obtained at various hydration times are depicted in Fig. 6. The resulting products align with the standard PDF card for 4-1-4 type basic magnesium carbonate. The peaks on each crystal surface show an increasing trend as the hydration time prolongs. Among them, the three more compact peaks corresponding to the (-4 1 3), (1 1 3), and (1 3 2) crystallographic facets seemed to be overlapping under the condition of a 1-hour hydration duration. Meanwhile, the three peaks corresponding to the (-3 2 1), (2 3 0), and (4 0 0) crystallographic facets at 30-40 degrees were not clearly visible, possibly indicating incomplete crystallization. The peak intensities of the two primary crystal faces, (0 1 1) and (3 1 0), exhibit a pattern of increasing and then decreasing.

Compared to scanning electron microscopy (SEM), the peak intensity of each crystal surface is lower, and the corresponding shape of magnesium alkali carbonate is irregular when the hydration time is 1 hour. After 1.5 hours of hydration, the degree of exposure of each crystal surface increases, leading to the transformation of the overall magnesium alkali carbonate into a rosette shape with a higher degree

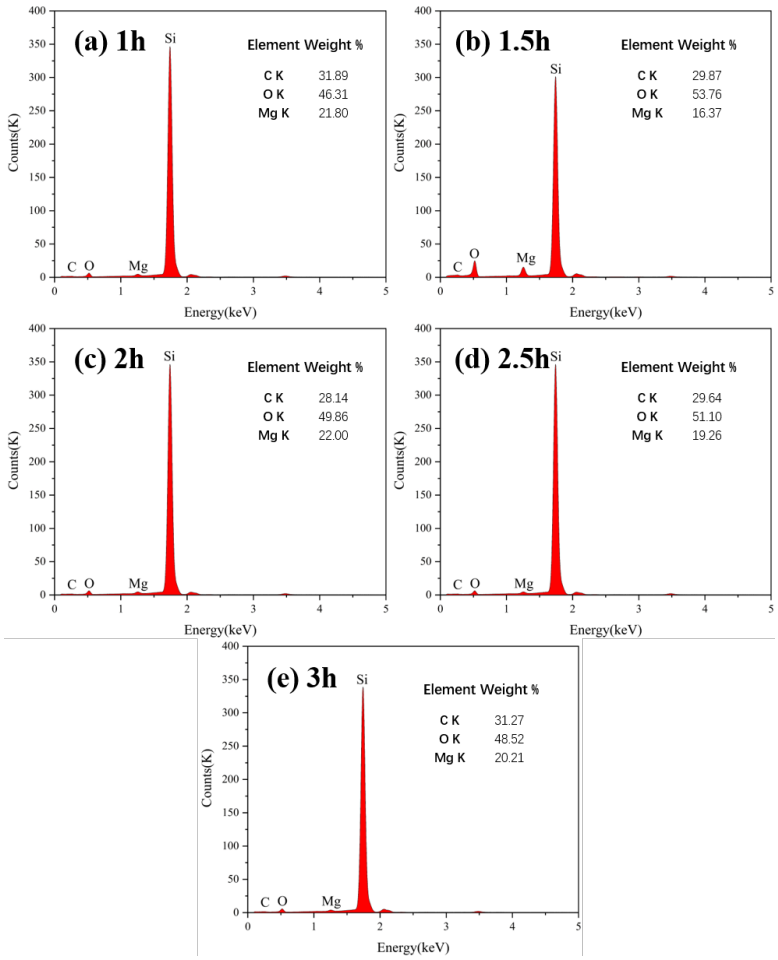

Fig. 6. EDS images of alkaline magnesium carbonate obtained at different hydration times

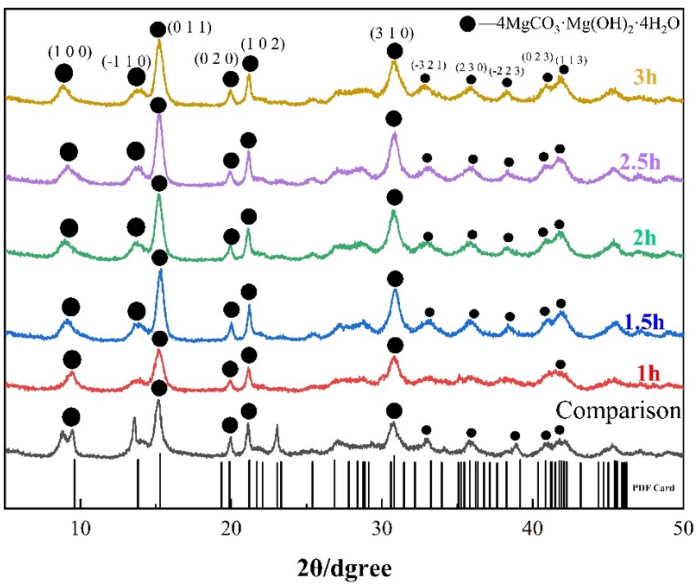

Fig. 7. XRD of basic magnesium carbonate obtained by different hydration time

of interspersal between petals. Extending the hydration time to 3 hours leads to a reduction in the XRD peak intensity of each crystal surface and disrupts the overall morphology of the sample, causing it to no longer resemble a flower ball in shape. This could be attributed to the larger size of the magnesium hydroxide nuclei, which is a result of the extended hydration time. Additionally, the surface carbonization is transformed into free magnesium ions, which enhances the final carbonization degree

of each crystal surface. The material belongs to the monoclinic structure, ideally forming hexagonal lamellae with stronger bonding energy in the (100) and (001) facets and a lower density of facet network. According to the crystallographic orientation and the magnitude of the interfacial energy of the crystal faces, the growth mainly occurs along these two crystal faces during the process of crystallization growth (Chen et al., 2016).

The XRD and SEM results indicate that prolonging the hydration time deepens the hydration of magnesium oxide. This may be due to the gradual increase in the exposed area of the dominant crystal surface of magnesium hydroxide, which affects the carbonization efficiency and alters the precursor liquid magnesium bicarbonate concentration of magnesium alkali carbonate, ultimately resulting in differences in the morphology of magnesium alkali carbonate.

3.2. Influence of hydration temperature on the morphology control of basic magnesium carbonate in hydration-carbonation

The results of X-ray diffraction (XRD) and scanning electron microscopy (SEM) analyses of alkaline magnesium carbonate products produced at different hydration temperatures for a hydration time of 1.5 h are shown in Figs. 8 and 10, respectively.

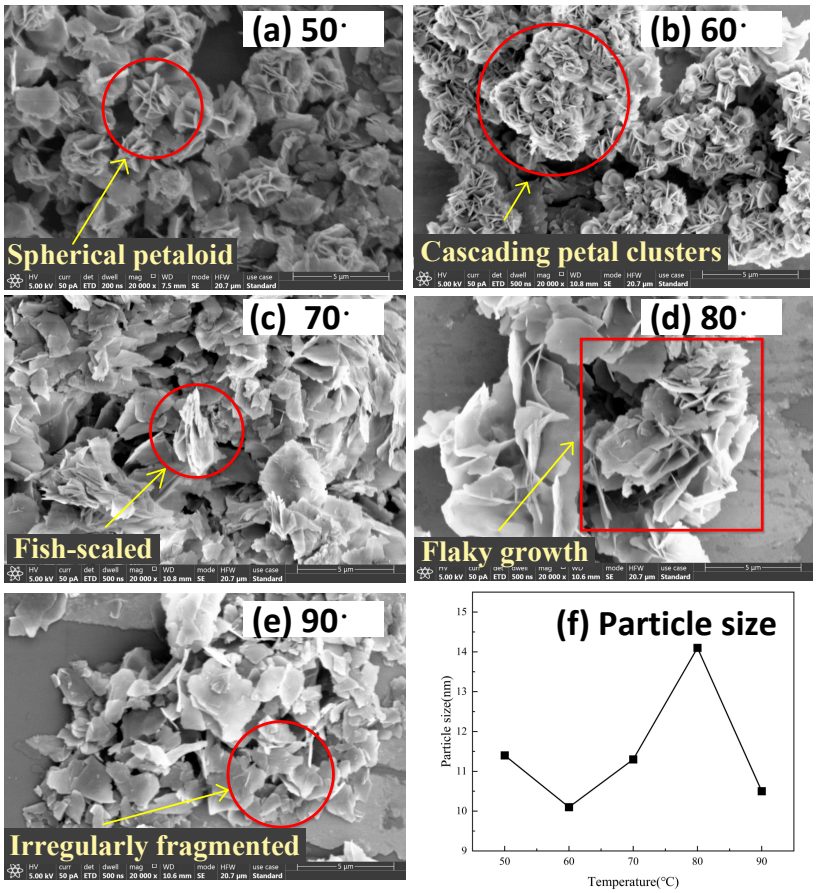

Fig. 8. SEM of basic magnesium carbonate at different hydration temperatures

Figs. 8(a) through 8(e) demonstrate that the morphology of the magnesium carbonate samples hydrated at 50°C is similar to petal-like spherical crystals. When the hydration temperature was increased to 60°C, the petal-like spherical magnesium carbonate agglomerated, and the volume of lamellae decreased while the number of overlapped layers significantly increased. Upon further heating to 70°C, the overlapping of the lamellae intensified, causing the magnesium carbonate to transform from petal-shaped spherical crystals to a fish-scale distribution. At 80°C, the overlapping of the lamellae decreased, leading to an increase in area and the formation of large-area lamellae. Continuing to heat the mixture to 90°C caused the magnesium carbonate alkali to break down into a regular shape.

As shown in Fig. 8(f), the effect of hydration duration on particle size differs from that of hydration temperature. The latter shows a pattern of decreasing, increasing, and then decreasing again. As the temperature of hydration increases, the crystal growth of magnesium hydroxide becomes more refined. Consequently, the area of the exposed crystal surface gradually increases under the same carbonization conditions, and the overall reaction with carbon dioxide exhibits an increasing trend. However, the Mg^{2+} ions generated by the dissolution of magnesium oxide mostly adsorb onto the surface of magnesium oxide particles, forming a nucleus for growth. As the temperature increases, the phenomenon of in-situ growth of magnesium hydroxide becomes increasingly serious. The particles grow larger due to hydration, and a small amount of magnesium hydroxide forms freely in solution, resulting in a wide range of particle sizes (Wang, 2020). The variation in growth rates among crystal surfaces results in differences in carbonation rate, crystallinity of Mg(OH)2, and activation energy of the reaction. This challenge arises from the requirement to separate well-crystallized Mg(OH)2, which demands a higher activation energy (Zhai et al., 1996). As a result, the particle size distribution of the final product shows this trend.

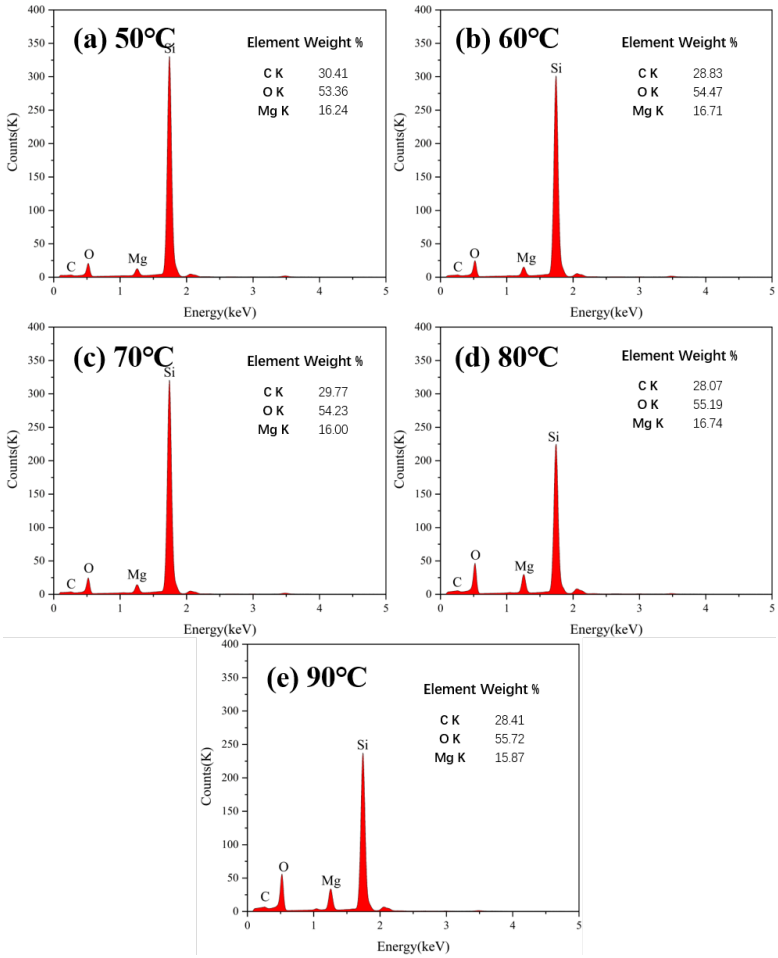

Fig. 9. EDS images of alkaline magnesium carbonate obtained at different hydration temperatures

The EDS analysis results for samples obtained at different hydration temperatures are shown in Fig. 9. Compared to the background peak intensity at the same hydration temperature, there is a certain degree of decrease, while the peak intensities corresponding to C, O, and Mg elements show varying degrees of increase. The carbon content decreases with increasing hydration temperature. At a hydration temperature of 90°C, the Mg element content is the lowest, with magnesium mass around 16%, and there are no other impurities present.

Fig. 10 shows a significant increase in the peaks of the (0 1 1) crystalline facets after the temperature was raised to 80°C, consistent with the expected trend. Similarly, increasing the hydration temperature to 60°C led to a notable increase in the peak intensities of the crystal faces, with even higher intensities

for specific crystal faces. The samples also seemed to be agglomerated. In particular, the crystal faces (-3 2 1), (2 3 0), (-2 2 3), and (1 1 3) showed significant enhancement. In contrast, the accompanying peaks of polycrystalline facet mixing near 41 degrees appeared to be weakened at 90°C. This weakening may be one of the reasons for the fragmentation of the samples under the corresponding conditions.

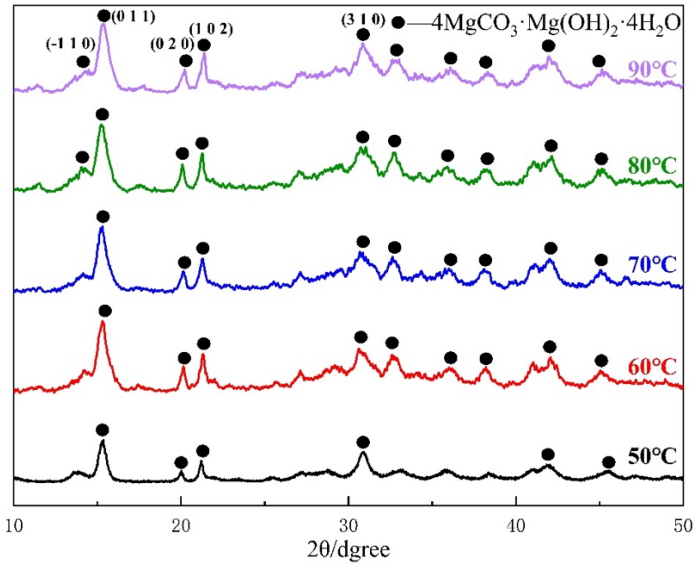

Fig. 10. XRD of alkaline magnesium carbonate at different hydration temperatures

3.3. Mechanistic analysis of the hydration-carbonation process

To improve the understanding of adsorption during the hydration-carbonation treatment process at the molecular level, we developed a hydration-carbonation adsorption model using molecular simulation (MS) software. The model takes into account the surface energy and water molecule adsorption energy of magnesium oxide, as well as the carbon dioxide adsorption energy of magnesium hydroxide. The study investigated the concentration of magnesium bicarbonate, the order of hydration preference at each crystalline surface of magnesium oxide, and the interaction between the hydration and carbonation processes by calculating the corresponding adsorption model for both.

3.3.1. Mechanistic analysis of the hydration-carbonation process

The magnesium oxide model diagram in Fig. 9 was calculated using the cell model in Fig. 2. This model roughly illustrates the distribution of each crystal surface. The hydration process of magnesium hydroxide is influenced by the particle size of the magnesium oxide particles and the extent of the hydration reaction on each crystal surface of magnesium oxide. In contrast, magnesium oxide is produced from various sources of magnesium, each with different lattice defects. As a result, the model does not show the labelling of the (2 2 0), (2 2 2), and (3 1 1) crystal planes.

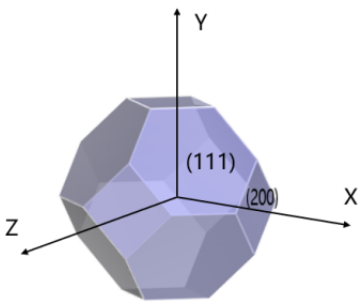

Fig. 11. Magnesium oxide crystal surface model

The Material Studio 2019 software was utilized to compute water adsorption on magnesium oxide (1 1 1), (2 0 0), (2 2 0), (3 1 1), and (2 2 2) surfaces using Simulated Annealing, Dynamics, and GGA-PBE

methods within the Adsorption, Forcite, and CASTEP modules. During the hydration of MgO, the E_{Ads}, E_{Total}, and related parameters at the crystal surfaces were analyzed, along with the molecular and radial distribution of water molecules around magnesium atoms. The interaction energy is calculated as follows:

$$E_{surf} = \frac{E_{Slab} - nE_{Bulk}}{2A} \quad (5)$$

where E_{slab} is the energy of the corresponding crystal surface, E_{bulk} is the energy of the cell as a whole, N is the ratio of the number of crystal faces to the number of cell atoms and A is the cross-sectional area of the crystal plane (Zhang et al. ,2014).

Table 2. Surface energy of each crystal surface of magnesium oxide

hkl	E_{Surf}/eV
(1 1 1)	0.36150881
(2 0 0)	0.20172878
(2 2 0)	0.14264379
(3 1 1)	0.12164703
(2 2 2)	0.34408612

Adsorption energy and surface energy are both crucial parameters in surface chemistry. Adsorption energy measures the ease of foreign atom adsorption on a surface, while surface energy measures the degree of stabilization of a structure before and after a reaction (Li et al., 2012). The higher the surface energy, the more difficult it is to create the corresponding solvation surface, leading to greater thermodynamic instability (Zhang et al., 2021). The Monte Carlo method was employed for the adsorption simulation calculations. This method is widely used in materials, chemistry, and physics to address the issue of random diffusion of molecules (Yang et al., 2020). Table 2 presents the correlation between the surface energy and the magnitude of each crystal surface of magnesium oxide. The stability of the crystallographic planes in magnesium oxide can be ranked as follows: E_{Surf}(2 0 0) > E_{Surf}(2 2 2) > E_{Surf}(1 1 1) > E_{Surf}(3 1 1) > E_{Surf}(2 2 0).

Upon comparing the X-ray diffraction (XRD) patterns of the raw materials, it was observed that the (3 1 1) and (2 2 0) crystallographic planes, which are relatively less exposed, are less stable than the more exposed (2 0 0) nonpolar planes. The (200) nonpolar planes are the most stable crystallographic planes exposed in magnesium oxide, with fewer lattice defects. The (1 1 1) crystal plane is less exposed but has a higher surface energy compared to a nonpolar plane. The crystalline surfaces of magnesium oxide (MgO) consist of alternating layers of metal and oxygen ions, creating perpendicular electrostatic dipole fields on the surface. The surface energy of the polar surfaces at the ends of the block depends on the thickness of the plate. Therefore, the polar surface of magnesium oxide has long been considered unstable (Zhang et al., 2008). At the same time, protonation of the (1 1 1) crystal surface stabilizes the MgO (1 1 1) surface and creates a structure resembling the solvation surface of the (0 0 1) crystal surface of magnesium hydroxide (Refson et al., 1995). The (1 1 1) and (2 2 2) facets are the most hydrophilic and have the strongest interaction forces with water molecules.

Fig. 12 illustrates that the (1 1 1), (3 1 1), and (2 2 2) crystalline surfaces, composed of magnesium ions as surface atoms, are polar surfaces. On the other hand, the (2 0 0) and (2 2 0) crystalline surfaces, which consist of oxygen and magnesium ions as surface atoms, are nonpolar surfaces. Based on surface energy calculations, the magnesium oxide raw material is more likely to agglomerate during the hydration process when the (3 1 1) crystalline surfaces are exposed.

Table 3. Adsorption energy and total energy of each crystal surface of magnesium oxide and water molecules

hkl	E_{Ads}/(kcal/mol)	E_{Total}/(kcal/mol)
(1 1 1)	-185.047233	-185.042164
(2 0 0)	-0.32130	-0.316230
(2 2 0)	-6.865159	-6.860090
(3 1 1)	-0.962991	-0.957922
(2 2 2)	14.862013	14.856945

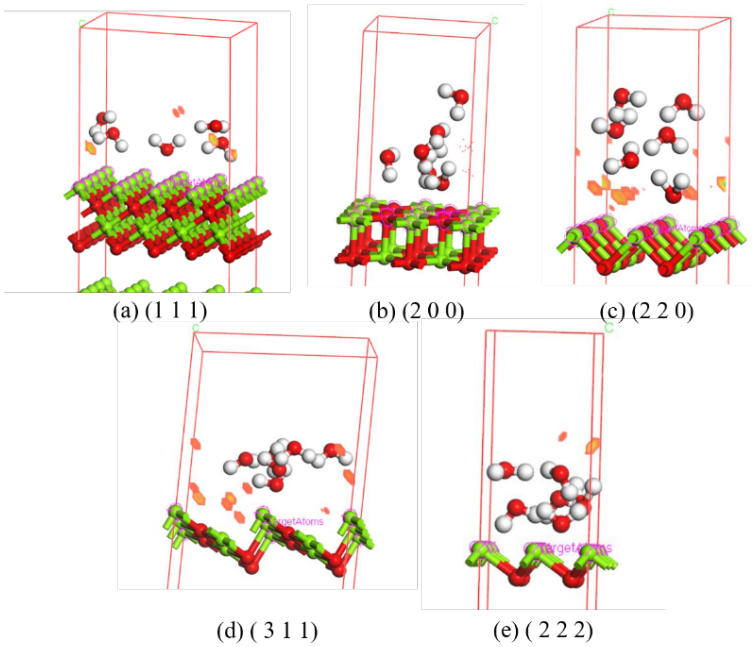

Fig. 12. Calculation model of the adsorption of water molecules on each crystalline surface of magnesium oxide

Table 3 presents the calculated magnitude relationship of water adsorption energy on each crystal surface of magnesium oxide using the Forcite module.E_{Ads}(1 1 1) < E_{Ads}(2 2 0) < E_{Ads}(3 1 1) < E_{Ads}(2 0 0) < E_{Ads}(2 2 2), while the total energy follows the order: E_{Total} (1 1 1) < E_{Total} (2 2 0) < E_{Total} (3 1 1) < E_{Total} (2 0 0) < E_{Total} (2 2 2). The results indicate that the (1 1 1) and (2 2 0) crystal surfaces are the most susceptible to the adsorption of water molecules and are the most stable after adsorption. The adsorption energy follows a specific order, which can be determined from the hydration adsorption energy, indicating the preference for the reaction of water molecules during the hydration of magnesium oxide. The differences in conclusions drawn from the surface energy could be attributed to the (2 2 0) crystalline surface being more distant from the other magnesium atoms compared to other crystalline surfaces. This makes it more susceptible to hydrolysis, adsorption of hydrogen atoms, and completion of the hydration reaction.

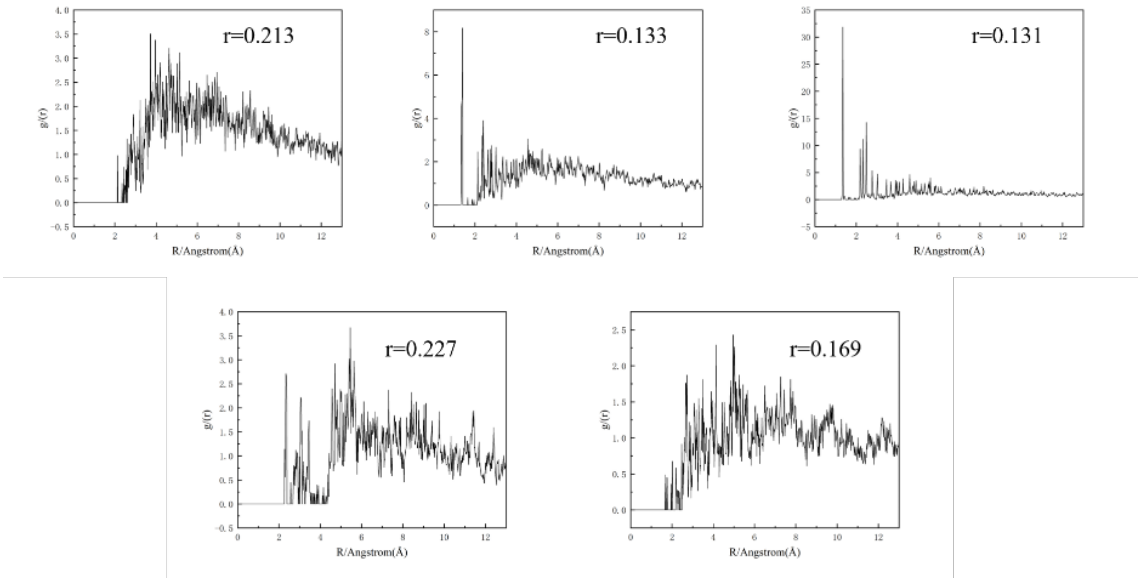

Fig. 13. Radial distribution functions of water molecules on different crystalline planes

The radial distribution function (RDF) represents the probability of finding the central particle within a sphere of radius r, while the other particles are present. The bond length of the corresponding

structure of the two particles can be determined by identifying the horizontal coordinate corresponding to the first peak of the g(r) curve (Yu et al., 2023). Fig. 11 illustrates that the distances between magnesium atoms and water molecules are greater in the (1 1 1) and (3 1 1) crystal faces, measuring 0.213 nm and 0.227 nm, respectively, compared to the other crystal faces, which have distances of less than 0.250 nm. This indicates that most of the water molecules in the surface layer of the crystals underwent a hydration reaction with magnesium atoms on the crystal faces, resulting in the formation of magnesium hydroxide on the surface of magnesium oxide.

3.3.2. Magnesium hydroxide carbonization adsorption energy

The process of magnesium hydroxide carbonation involves the transfer of carbon dioxide molecules from the gas phase to the gas-liquid interface, and then to the liquid phase. Additionally, it involves the dissolution of magnesium hydroxide and the diffusion of magnesium ions into the liquid phase. This is an interphase mass transfer process. According to the film-forming theory, the absorption of carbon dioxide is equivalent to molecular diffusion through gas-liquid membranes (Chen et al., 2022). While this process is influenced by the particle size, dissolved particle diameter, and the secondary chemical membrane reaction (Zhao et al., 2016), the reaction within this chemical membrane is elucidated by molecular dynamics.

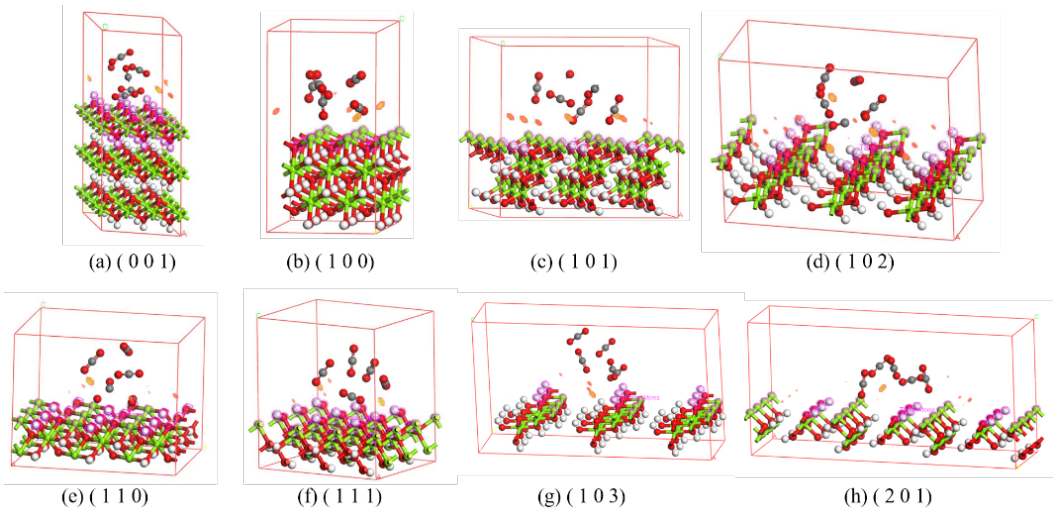

Fig. 14. Computational model of carbon dioxide molecule adsorption on each crystalline surface of magnesium hydroxide

Table 4 presents the correlation between the adsorption energy of carbon dioxide molecules on each crystal surface of magnesium hydroxide. The order of magnitude is as follows: E_{Ads}(1 0 2) < E_{Ads}(0 0 1) < E_{Ads}(2 0 1) < E_{Ads}(1 0 1) < E_{Ads}(1 1 0) < E_{Ads}(1 0 0) < E_{Ads}(1 0 3) < E_{Ads}(1 1 1). The most stable surfaces for adsorption are the crystalline surfaces (102), (001), (201), and (101). The (001) and (101) surfaces of magnesium hydroxide are the primary exposed crystalline surfaces. An increase in hydration temperature enhances the susceptibility of (001) crystalline surfaces to overcome the energy barrier (Zhao et al., 2014). This can have a significant impact on adsorption. The different levels of exposure of each crystal surface will lead to varying morphologies of magnesium hydroxide, thereby affecting the morphology of magnesium carbonate trihydrate (Cheng et al., 2019). This, in turn, will further influence the extent of crystallization of the final pyrolysis product, magnesium basic carbonate. The size of magnesium hydroxide particles increases with prolonged hydration time, which inhibits the growth of (0 0 1) crystalline facets (Liu et al., 1989). Consequently, a longer hydration time leads to a decreased proportion of (001) crystalline facets in the intermediate product of magnesium hydroxide.

Table 4 and Fig. 15 show that the (1 0 2) crystallite has the lowest adsorption energy and the most stable CO_2 adsorption, and corresponds to the largest probability of the radial distribution function. The value of g(r) exceeds 3% around 0.6 nm, which is higher than the adsorption probabilities of the other crystallites. The (0 0 1) and (1 0 3) crystallites have the smallest adsorption distances, which allows a higher rate of free magnesium ions in solution. The calculations support this possibility.

Table 4. Adsorption energy and total energy of each crystal plane of magnesium hydroxide and carbon dioxide

hkl	E_{Ads}/(kcal/mol)	E_{Total}/(kcal/mol)
(0 0 1)	-6.32598022	-6.32595198
(1 0 0)	-5.68281859	-5.68279035
(1 0 1)	-6.03658909	-6.03656084
(1 0 2)	-6.79866494	-6.79863669
(1 1 0)	-5.75047944	-5.75045119
(1 1 1)	-4.66759496	-4.66756672
(1 0 3)	-5.61455750	-5.61452926
(2 0 1)	-6.10907703	-6.10904878

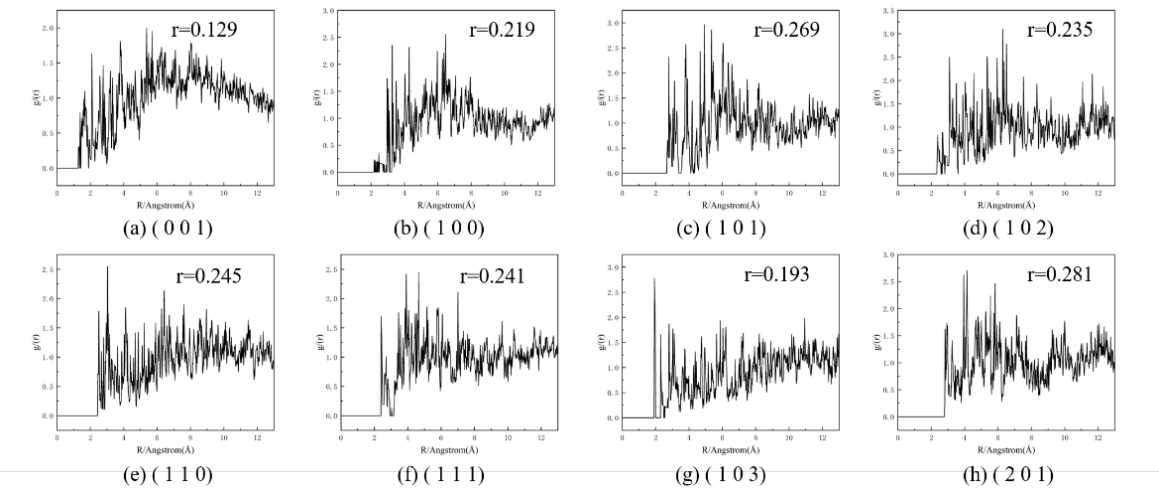

Fig. 15. Radial distribution functions of carbon dioxide molecules on different crystallographic planes

The surface energy relationship of magnesium oxide is as follows: E_{Surf}(3 1 1) < E_{Surf}(2 2 0) < E_{Surf}(2 0 0) < E_{Surf}(2 2 2) < E_{Surf}(1 1 1). During hydration, the (1 1 1) crystalline surface is the most reactive with water molecules. The more the (1 1 1) crystal surface is exposed, the faster the hydration reaction rate and the corresponding hydration temperature requirement is further reduced. Based on the XRD analysis of the raw material, it is evident that the (2 0 0) crystal surface is the most exposed. This surface has low surface energy and low adsorption energy for water molecules. Therefore, a higher hydration temperature will improve the efficiency of the hydration reaction and increase the concentration of magnesium bicarbonate. The hydration temperature has a significant effect on the Gibbs energy function for nucleation, leading to the formation of a large number of small-sized, low-crystallinity magnesium hydroxide crystals (YUAN et al., 2015).

The relationship between adsorption energy and magnesium hydroxide is as follows: E_{Ads}(1 0 2) < E_{Ads}(0 0 1) < E_{Ads}(2 0 1) < E_{Ads}(1 0 1) < E_{Ads}(1 1 0) < E_{Ads}(1 0 0) < E_{Ads}(1 0 3) < E_{Ads}(1 1 1). The stability of the bond between magnesium hydroxide and carbon dioxide increases as the adsorption energy increases. This reduces the likelihood that magnesium atoms will break away from the hydroxide structure and form weakly bonded carbonate and magnesium ions with carbon dioxide and water. As carbon dioxide continues to pass through the solution, the carbonate is gradually converted to bicarbonate, forming a suspension of magnesium bicarbonate dissolved in water after carbonation and magnesium hydroxide not yet carbonated. Therefore, lower adsorption energy corresponds to greater crystal surface exposure, resulting in a faster increase in magnesium bicarbonate concentration and overall carbonization efficiency. The final efficiency of carbonization depends on the dominance of magnesium hydroxide in crystal surface exposure and the density of the nuclei.

4. Conclusions

A magnesium bicarbonate solution with a concentration of 0.15 mol/L can be obtained by hydrating at a temperature of 50 ℃ for 1.5 hours. At this concentration, magnesium bicarbonate can be prepared as

spherical basic magnesium carbonate. The increase of hydration temperature will make the basic magnesium carbonate agglomeration phenomenon, and the prolongation of hydration time makes its particle size appear a certain degree of decline. Specifically, a concentration of 0.15 mol/L of magnesium bicarbonate solution results in relatively uniform particle size. However, further increases in concentration lead to a decrease in particle size and a loss of uniformity. Additionally, the overall morphology changes from a spherical shape to a fragmented shape. At the same time, the CASTEP module calculations reveal that among the magnesium oxide crystals, the (1 1 1) and (2 2 2) facets have higher surface energy, while the (3 1 1), (2 0 0), and (2 2 2) facets have weaker surface energy. The (1 1 1) and (2 2 2) crystalline surfaces, which contain the highest concentration of magnesium oxide, are the most susceptible to hydration during the hydration process. The Forcite module was used to identify the stable adsorption sites of water molecules in the early stages of magnesium oxide hydration. The degree of hydration of each crystal surface of magnesium oxide deepened gradually in the sequence of (1 1 1), (2 2 0), (3 1 1), (2 0 0), and (2 2 2), resulting in the formation of various pre-positioned materials of magnesium hydroxide. The (1 0 2) crystalline surface of magnesium hydroxide exhibits the highest carbonation performance, and the carbonation of each crystalline surface gradually transforms into free magnesium ionic groups in the following order: (1 0 2), (0 0 1), (2 0 1), (1 0 1), (1 1 0), (1 0 3), (1 1 1). Both the primary exposed crystal surfaces of magnesium hydroxide, (0 0 1) and (1 0 1), are prone to stable adsorption of carbon dioxide. The degree of crystallization of magnesium hydroxide and the density of the nuclei affects the concentration of magnesium bicarbonate, ultimately contributing to the differences in the morphology of magnesium alkali carbonate.

Acknowledgments

The authors thank the Natural Science Foundation of Hebei Province (Iron and Steel Joint) Project (E2022209127), the Science and Technology Research Program of Higher Education Institutions of Hebei Province (CXY2023008), and the Youth Fund for Scientific Research of Higher Education Institutions of Hebei Province Project (QN2024215) for providing all the facilities for the development of this study.

References

BOTHA, A., STRYDOM, C., 2001. *Preparation of a magnesium hydroxy carbonate from magnesium hydroxide*. Hydrometallurgy. Hydrometallurgy, 62(3), 175-183.

CHEN, J., HUANG, X, Y., HUANG, Z, L., 2016. *Effect of different alkali sources on crystal form of basic magnesium carbonate*. Material Protection. 49(S1), 196-197.

CHEN, M.M, YU-ZHU SUN, XING-FU SONG, ET AL, 2022. *Study on the carbonization process of magnesium hydroxide[J]*. Journal of East China University of Science and Technology (Natural Science Edition), 48(05), 600-608.

CHEN, G, L., SONG, X, F., XU, Y, X., YU, J, G., 2017. *Effects of NO_3^- and SO_4^{2-} ions on the coupled reaction–extraction–crystallization process of $MgCl_2$ and CO_2*. Ind. Eng. Chem. Res. 56 (2017) 7100−7108

CHEN, Y., Huang, X, Y., 2016. Effect of different alkali sources on the crystal shape of basic magnesium carbonate. Materials Protection.

CHENG W, T., FANG, L., CHENG, H, G., 2019. *Formation of $MgCO_3·3H_2O$ in the CO_2 mineralization system using $Mg(OH)_2$ as an intermediate at 20 ℃*. Journal of Industrial and Engineering Chemistry, 76, 215-222.

H.T. SCHAEF., C.F. WINDISCH JR., B.P. MCGRAIL., P.F. MARTIN., K.M. ROSSO., 2011. *Brucite [$Mg(OH)_2$] carbonation in wet supercritical CO2: an in situ high-pressure X-ray diffraction study*. Geochim. Cosmochim. Ac. 75 (2011) 7458−7471.

HUANG J, C., LIN, G, S., ZONG, J. et al, 2021. *Exploration of new process conditions for the preparation of highly dispersed hexagonal flake nano-magnesium hydroxide from hydromagnesite*. Inorganic Salt Industry, 53(02), 55-60.

LI, J., YANG, Y., LUO, X., 2012. *First-principles study of the Al(001)/Al3 Ti(001) interfacial properties.* Computational Materials Science, 62.

KYUNGIL, C., YERYEONG, K., SUKBYUNG, C., 2023. *Forced Mineral Carbonation of MgO Nanoparticles Synthesized by Aerosol Methods at Room Temperature.* Nanomaterials, 13(2) :281-281.

LIU, B, Y., ZHOU, X, T., CUI X, S, TANG, J., 1989. *Synthesis of MgCO_3-5H_2O crystals and study of its crystal structure*. Chinese Science (Series B Chemistry Life Science Geology) (12),1302-1308.

MITSUHASHI, K.，TAGAMI, N.，TANABE, K.，2005，et al．*Synthesis of microtubes with a surface of " house of cards" structure via needlelike particles and control of their pore size*． Langmuir，21(8), 3659－3663．

REFSON, K., WOGELIUS, R.A., FRASER, D.G., PAYNE, M.C., LEE, M., MILMAN, V., 1995. *Water chemisorption and reconstruction of the MgO surface*. Physical review. B, Condensed matter, 52 15, 10823-10826.

SATO, T., Y, S, I, N., 2020.*Hydrothermal carbon dioxide fixation in magnesium hydroxide and serpentine: Effects of temperature and pH*.The Journal of Supercritical Fluids(prepublish),105071-.

STEFÁNSSON, A., LEMKE, H, K., BÉNÉZETH, P., ET AL, 2017. *Magnesium bicarbonate and carbonate interactions in aqueous solutions: An infrared spectroscopic and quantum chemical study*. Geochimica et Cosmochimica Acta. 198.

SUN, B, C., ZHOU H, J., MOSES A., J, M., CHEN, J, F., CHEN L, S., 2015. *Preparation of basic magnesium carbonate by simultaneous absorption of NH 3 and CO 2 into $MgCl_2$ solution in an RPB*. Powder Technology, 57-62.

V.R. CHOUDHARY, M.Y. PANDIT, 1991.*Surface properties of magnesium oxide obtained from magnesium hydroxide: Influence on preparation and calcination conditions of magnesium hydroxide*. Applied Catalysis, 71: 265-274.

WANG, D., 2020, *Hydration preparation and hydrophobic properties of two-dimensional nano-magnesium hydroxide*. North China University of Science and Technology.

WANG, Y,L., 2015. *Preparation and application study of micro/nano hydrated magnesium carbonate*. Northeastern University.

WANG, Y, L., YIN W, Z., LI, C., et al, 2020. *Surface organic modification and property characterization of basic magnesium carbonate*. Journal of the Chinese Ceramic Society. 48(01),120-127.

WU, S, N., T, B, T, S, Hasanthi L., W, P., 2021. *Polarization of CO2 for improved CO2 adsorption by MgO and $Mg(OH)_2$*. Applied Surface Science. 562.

YANG, F., FANG, X, H., ZENG, F, G., et al，2020. *Simulation calculation of adsorption of lead and cadmium on kaolinite surface*. Comprehensive utilization of minerals, (05), 196-202+100.

YU, L, L., LIU, J, X., QU, W, W., 2023. *Molecular simulation of O2 adsorption behavior on Ag surface*. Special Casting and Nonferrous Alloys, 43(11), 1447-1451.

YUAN, Q., LU, Z., ZHANG, P., ET AL., 2015. *Study of the synthesis and crystallization kinetics of magnesium hydroxide*. Materials Chemistry and Physics, 162734-742.

ZHAI, X, L., ZHOU, X, T., LIU, B, N., ET AL, 1996. *The influence of the crystallinity and particle size of $Mg(OH)_2$ on carbonation III. Research on the mechanism of carbonation reaction.* Inorganic Salt Industry. (06), 9-11.

ZHANG, D., ZHANG, P., SONG, S., ET AL., 2014. *Simulation of magnesium hydroxide surface and interface*. Journal of Alloys and Compounds, 612315-322.

ZHANG, H., XU, Z., CHEN, D., BO, H., ZHOU, Q., CHEN, S., LI, S., SUN, W., ZHANG, C., 2021. *Adsorption mechanism of water molecules on hematite (1 0 4) surface and the hydration microstructure*. Applied Surface Science, 550, 149328.

ZHANG, W., TANG, B., 2008. Stability of MgO(111) Polar Surface: Effect of the Environment. *Journal of Physical Chemistry C*, 112, 3327-3333.

ZHANG, L, L., LIU, J, X., L, M., 2008. *Effects of different pyrolysis conditions on the morphology of basic magnesium carbonate crystals (In English)*. Journal of Silicate. No. 233(09), 1310-1314.

ZHAO, B., MA, X, Q., BAI, Y., et al., 2017. *Study on the reaction of magnesium sulfate with sodium carbonate to prepare basic magnesium carbonate.* Inorganic salt industry, 49(09), 21-25.

ZHAO, W., HAN B., JAKOBSSON, K., ET AL., 2016. *Mathematical model of precipitation of magnesium carbonate with carbon dioxide from the magnesium hydroxide slurry*. Computers and Chemical Engineering, 87180-189.

ZHAO, Z, Y., LI X, G., WANG S. R., XIAO, Y., 2014. *Study on the preferential growth conditions of hexagonal lamellar magnesium hydroxide (001) crystal faces*. Journal of Artificial Crystals, 43(07), 1611-1619.

ZHU, C., WANG, H., Li, G, 2017. *CO_2 Absorption and Magnesium Carbonate Precipitation in $MgCl_2$–NH_3–NH_4Cl Solutions: Implications for Carbon Capture and Storage*. Minerals, 7(9), 172.